



# Moxidectin and Ivermectin Inhibit SARS-CoV-2 Replication in Vero E6 Cells but Not in Human Primary Bronchial Epithelial Cells

Nilima Dinesh Kumar,<sup>a,b</sup> Bram M. ter Ellen,<sup>b</sup> Ellen M. Bouma,<sup>b</sup> Berit Troost,<sup>b</sup> Denise P. I. van de Pol,<sup>b</sup> Heidi H. van der Ende-Metselaar,<sup>b</sup> Djoke van Gosliga,<sup>c</sup> Leonie Apperloo,<sup>d</sup> Orestes A. Carpaj,<sup>e</sup> Maarten van den Berge,<sup>e</sup> Martijn C. Nawijn,<sup>d</sup> Ymkje Stienstra,<sup>f</sup> Izabela A. Rodenhuis-Zybert,<sup>b</sup>  Jolanda M. Smit<sup>b</sup>

<sup>a</sup>Department of Biomedical Sciences of Cells & Systems, University Medical Center Groningen, University of Groningen, Groningen, The Netherlands

<sup>b</sup>Department of Medical Microbiology and Infection Prevention, University Medical Center Groningen, University of Groningen, Groningen, The Netherlands

<sup>c</sup>Department of Pediatrics, Beatrix Children's Hospital, University Medical Center Groningen, University of Groningen, GRIAC Research Institute, Groningen, The Netherlands

<sup>d</sup>Department of Pathology and Medical Biology, University Medical Center Groningen, University of Groningen, GRIAC Research Institute, Groningen, The Netherlands

<sup>e</sup>Department of Pulmonary Diseases, University Medical Center Groningen, University of Groningen, GRIAC Research Institute, Groningen, The Netherlands

<sup>f</sup>Department of Internal Medicine/Infectious Diseases, University Medical Center Groningen, University of Groningen, Groningen, The Netherlands

Nilima Dinesh Kumar, Bram M. ter Ellen and Ellen M. Bouma contributed equally to this work, and Izabela A. Rodenhuis-Zybert and Jolanda M. Smit contributed equally to this work. Author order was determined based on contribution to preparing the manuscript.

**ABSTRACT** Antiviral therapies are urgently needed to treat and limit the development of severe COVID-19 disease. Ivermectin, a broad-spectrum anti-parasitic agent, has been shown to have anti-SARS-CoV-2 activity in Vero cells at a concentration of 5  $\mu$ M. These limited *in vitro* results triggered the investigation of ivermectin as a treatment option to alleviate COVID-19 disease. However, in April 2021, the World Health Organization stated the following: "The current evidence on the use of ivermectin to treat COVID-19 patients is inconclusive." It is speculated that the *in vivo* concentration of ivermectin is too low to exert a strong antiviral effect. Here, we performed a head-to-head comparison of the antiviral activity of ivermectin and the structurally related, but metabolically more stable moxidectin in multiple *in vitro* models of SARS-CoV-2 infection, including physiologically relevant human respiratory epithelial cells. Both moxidectin and ivermectin exhibited antiviral activity in Vero E6 cells. Subsequent experiments revealed that these compounds predominantly act on the steps following virus cell entry. Surprisingly, however, in human-airway-derived cell models, both moxidectin and ivermectin failed to inhibit SARS-CoV-2 infection, even at concentrations of 10  $\mu$ M. These disappointing results call for a word of caution in the interpretation of anti-SARS-CoV-2 activity of drugs solely based on their activity in Vero cells. Altogether, these findings suggest that even using a high-dose regimen of ivermectin, or switching to another drug in the same class, is unlikely to be useful for treatment of SARS-CoV-2 in humans.

**KEYWORDS** moxidectin, ivermectin, antiviral, SARS-CoV-2, ALI, *in vitro*

Within less than 1.5 years, the pandemic SARS coronavirus 2 (SARS-CoV-2) has infected over 153 million individuals and resulted in over 3.2 million deaths worldwide (1–3). The social and economic burden of this still-ongoing pandemic is staggering, and, besides vaccine development, it is of utmost importance to develop therapeutic interventions to reduce disease symptoms. To date, multiple compounds have been shown to exert SARS-CoV-2 antiviral activity *in vitro* and several compounds have reached clinical trials (4, 5). Remdesivir and hydroxychloroquine were thought to be effective early in the pandemic, but after a careful evaluation in an interim solidarity trial, the WHO released a conditional yet strong recommendation against the usage of

**Copyright** © 2022 American Society for Microbiology. All Rights Reserved.

Address correspondence to Jolanda M. Smit, jolanda.smit@umcg.nl.

**Received** 4 August 2021

**Returned for modification** 27 September 2021

**Accepted** 8 October 2021

**Accepted manuscript posted online** 11 October 2021

**Published** 18 January 2022

these drugs as no impact on overall mortality was observed (6). Corticosteroids are currently (as of April 29, 2021) the only therapeutic agent strongly recommended by the WHO for the treatment of severe and critical COVID-19 patients (7). These guidelines, however, differ from National Institute of Health (NIH) guidelines, which recommend anti-SARS-CoV-2 monoclonal antibodies for selective patients with mild to moderate disease, and remdesivir, dexamethasone, and tocilizumab either individually or in combination based on disease severity (8).

Ivermectin, a macrocyclic lactone of the avermectin subfamily, is a broad-spectrum anti-parasitic agent approved by the United States Food and Drug Administration (FDA) and European Medicines Agency (EMA) for prophylactic and therapeutic usage in some animal species and for selective treatments in humans (9–12). In recent years, ivermectin has also been shown to have antiviral activity *in vitro* toward several viruses including Zika virus (ZIKV) and dengue virus (DENV) (13–17). In addition, Caly and colleagues (18) showed that ivermectin effectively inhibits SARS-CoV-2 infection in Vero/hSALM cells. However, the success of ivermectin as an antiviral agent *in vitro* has been proven difficult to translate to *in vivo* settings. For example, ivermectin failed to protect against lethal ZIKV challenge in mice (19) and did not reduce DENV viremia in phase III clinical trials (20). It is speculated that the *in vivo* concentration of ivermectin is too low to exert its antiviral effect (21, 22). Notably, despite the known limitations of achieving high ivermectin concentrations in humans (23, 24) and the limited *in vitro* proof of anti-SARS-CoV-2 activity (18), 65 ivermectin clinical trials (April 29, 2021) are registered for treatment intervention against COVID-19 (25). Recently, upon review of the latest trial results, many regulatory authorities, including the WHO, issued a recommendation “to not use ivermectin in patients with COVID-19 except in the context of a clinical trial,” as the available evidence to support its usage is uncertain (26–29).

Moxidectin, a macrocyclic lactone that belongs to the milbemycin subfamily and is structurally related to ivermectin, is a broad-spectrum anti-parasitic agent used in veterinary medicine. In addition, it has recently been approved for human use for the prevention of river blindness, a disease caused by the parasite *Onchocerca volvulus* (30–32). Importantly, moxidectin has been shown to have superior drug disposition properties when compared to ivermectin, such as a longer half-life and higher efficacy in animals and humans (31, 33). To date, the antiviral potential of moxidectin toward SARS-CoV-2 has not been evaluated and no clinical trials are registered for moxidectin as a COVID-19 treatment.

In this study, we evaluated the antiviral activity of moxidectin compared with ivermectin toward SARS-CoV-2 infection *in vitro*. We utilized the commonly used African green monkey kidney cells (Vero E6) to compare the effective antiviral concentrations of each compound and to evaluate their longevity and mechanistic properties. To verify the results in a physiologically more relevant model system, we subsequently tested the antiviral activity of both drugs in human lung epithelial cells (Calu-3) and in primary human bronchial epithelial cells (PBECS) grown under air-liquid interface (ALI) culture conditions (34).

## RESULTS

**Moxidectin and ivermectin inhibit SARS-CoV-2 infection in Vero E6 cells.** First, we assessed the antiviral activity of moxidectin toward SARS-CoV-2 in the African green monkey kidney epithelial Vero E6 cell line and compared that to the efficacy of ivermectin. Vero E6 is highly permissive to SARS-CoV-2 infection (35) and thus commonly used in studies investigating virus-host interactions and potential antiviral drugs. Prior to assessing the antiviral efficacy, we determined the cellular cytotoxicity of moxidectin and ivermectin in Vero E6 cells. A clear dose-dependent cytotoxicity was observed (see Fig. S1 in the supplemental material) with a  $CC_{50}$  value of 30.4  $\mu$ M for moxidectin and 36.4  $\mu$ M for ivermectin. The highest nontoxic dose was set at 10  $\mu$ M for subsequent experiments. At this concentration, the cell viability was above 90% for both moxidectin (see Fig. S1A) and ivermectin (see Fig. S1B). Next, Vero E6 cells were

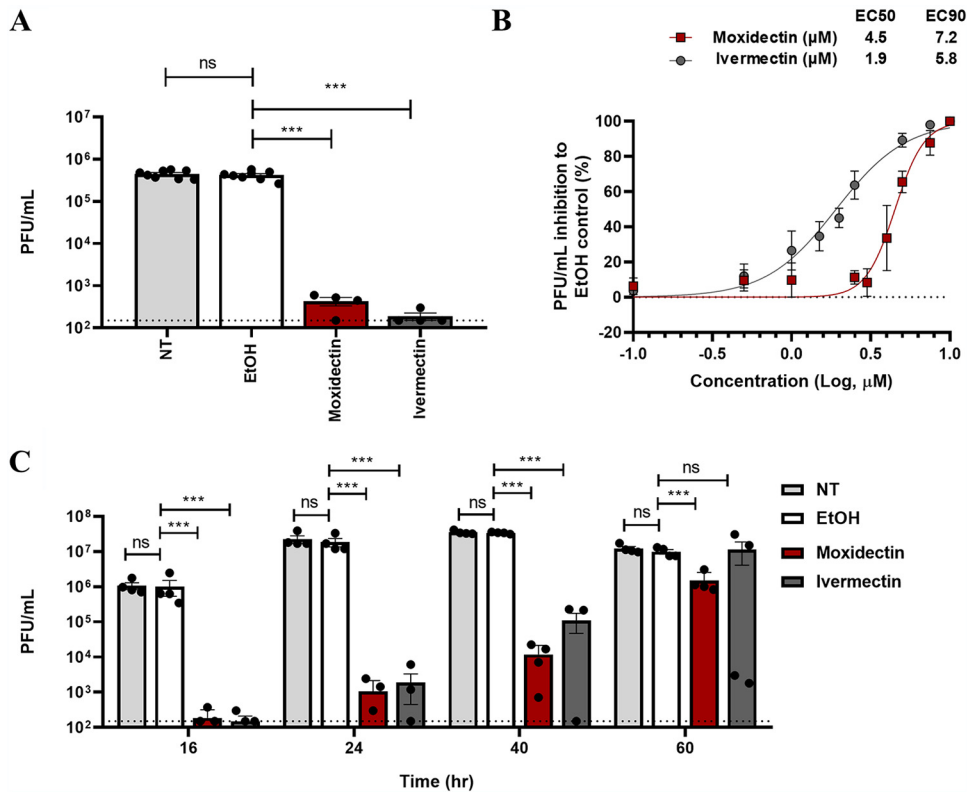


**FIG 1** Antiviral activity of moxidectin and ivermectin toward SARS-CoV-2 in Vero E6 cells. Vero E6 cells were treated with 10 μM moxidectin or ivermectin in the presence of SARS-CoV-2 at MOI 1. At 2 h postinfection (hpi), cells were washed twice with plain DMEM, new cell culture medium containing the compound was added, and incubation was continued for another 6 h. At 8 hpi, cell supernatants were harvested and the number of produced infectious virus particles was determined by plaque assay. (B) Vero E6 cells were treated with increasing concentrations of moxidectin or ivermectin and infection was continued as described for panel A. The EC<sub>50</sub> and EC<sub>90</sub> values were calculated using GraphPad Prism software. (C) Antiviral effect of 10 μM moxidectin or ivermectin or the corresponding volume of EtOH at 16, 24, 40, and 60 hpi. Dotted lines indicate the detection limit of plaque assay. Each dot represents data from a single independent experiment. Data for at least three independent experiments are represented as mean ± SEM. Statistical analysis was carried out by comparing treated samples with the EtOH control using a Student's *t* test. \*\*\* (*P* < 0.001), \*\* (*P* < 0.01), \* (*P* < 0.05), and "ns" (nonsignificant).

infected with SARS-CoV-2 at a multiplicity of infection (MOI) of 1 in the presence of 10 μM moxidectin and ivermectin, or the equivalent volume of EtOH, and virus progeny was determined at 8 hours post-infection (hpi). This time point corresponds to 1 cycle of replication (36). SARS-CoV-2 infection under non-treated (NT) conditions led to a production of  $4.9 \pm 0.8 \times 10^5$  PFU/ml (Fig. 1A). A comparable titer was observed for the EtOH control ( $4.3 \pm 0.7 \times 10^5$  PFU/ml), indicating that the solvent does not influence infectious virus particle production. In line with previous results (18), ivermectin was found to exert significant antiviral activity toward SARS-CoV-2 in Vero E6 cells (Fig. 1). In the presence of 10 μM ivermectin, infectious virus particle production was reduced to  $1.9 \pm 0.8 \times 10^2$  PFU/ml, which corresponds to a reduction of more than 99.9% compared to the EtOH control (Fig. 1A). In the presence of 10 μM moxidectin, the infectious virus titer was reduced to  $4.3 \pm 2.0 \times 10^2$  PFU/ml, which also corresponds to a reduction of 99.9% compared to the EtOH control (Fig. 1A). Next, we performed a dose-response analysis to determine the EC<sub>50</sub> and EC<sub>90</sub> values (i.e., a reduction of 50% and 90% in viral titer, respectively). To this end, Vero E6 cells were infected with SARS-CoV-2 in the presence of increasing concentrations of both moxidectin, ivermectin, and the corresponding amount of EtOH. Moxidectin and ivermectin showed a dose-dependent antiviral activity in Vero E6 (Fig. 1B), with an EC<sub>50</sub> and EC<sub>90</sub> of 4.5 μM and 7.2 μM for moxidectin and 1.9 μM and 5.8 μM for ivermectin,

respectively (Fig. 1B). The observed  $EC_{50}$  for ivermectin is in line with the previously published value of  $\sim 2 \mu\text{M}$  (18). Thus, both compounds exhibit potent antiviral effects toward SARS-CoV-2, with ivermectin being slightly more potent than moxidectin in this experimental set-up.

Given the known increased stability of moxidectin over ivermectin, we next evaluated the durability of the antiviral effect for both compounds. To this end, Vero E6 cells were infected with SARS-CoV-2 at MOI 0.01 in the presence of  $10 \mu\text{M}$  moxidectin, ivermectin, or corresponding amount of EtOH, and the cell supernatants were harvested at 16, 24, 40 and 60 hpi. These time points roughly correspond to 2, 3, 5, and 7 SARS-CoV-2 replication cycles, respectively (36). Importantly, the prolonged incubation of the cells with moxidectin and ivermectin did not influence cell viability as measured with the MTS assay (see Fig. S1C). At 40 hpi,  $3.5 \pm 0.4 \times 10^7$  PFU/ml was produced in non-treated infection conditions, at which point virus particle production reached its plateau (Fig. 1C). Comparable titers were observed over time for the EtOH control ( $3.4 \pm 0.2 \times 10^7$  PFU/ml at 40 hpi), indicating that EtOH had no effect on virus progeny production. More than 100-fold reduction in virus particle production was observed at 16, 24, and 40 hpi following infection in the presence of moxidectin or ivermectin (Fig. 1C). At 60 hpi, ivermectin showed antiviral activity in 2 experiments, yet there was considerable variation between the other 2 experiments and therefore no significant antiviral effect was seen. In contrast, a moderate but consistent antiviral effect of moxidectin was seen at 60 hpi. At this time point, the titer reduced from  $9.9 \pm 2.9 \times 10^6$  PFU/ml (EtOH control) to  $1.5 \pm 1.0 \times 10^6$  PFU/ml, which corresponds to a reduction of 84.8%. In conclusion, a single  $10 \mu\text{M}$  dose of both compounds controlled SARS-CoV-2 replication for at least 5 replication cycles. For moxidectin, a more consistent antiviral effect was observed, lasting until 7 replication cycles.

**Moxidectin and ivermectin interfere with SARS-CoV-2 replication.** To delineate the mode of action of each drug, we first investigated whether moxidectin and ivermectin exhibit a direct virucidal effect. To this end,  $10 \mu\text{M}$  moxidectin, ivermectin, or the corresponding amount of EtOH control was incubated with  $2.5 \times 10^5$  SARS-CoV-2 particles at  $37^\circ\text{C}$  for 2 h and the infectious titer was determined by plaque assay. The highest concentration in the diluted sample corresponded to  $1 \mu\text{M}$  compound; at this concentration, no antiviral effect in Vero E6 cells was observed (Fig. 1B), and therefore the plaque assay can be used as a readout. Importantly, no differences in viral titer were observed between the moxidectin- or ivermectin-treated samples and the EtOH control (Fig. 2A), indicating that these compounds do not exhibit virucidal activity to SARS-CoV-2 particles. Next, we performed a time-of-drug-addition assay. Here,  $10 \mu\text{M}$  moxidectin or ivermectin was administered either prior to virus inoculation, during virus inoculation, or post-virus inoculation (Fig. 2B). Cells were infected with SARS-CoV-2 at an MOI of 1 and supernatants were collected at 8 hpi to determine progeny infectious virus particle production. Each treatment included a corresponding EtOH control. No effect on the viral titers was observed when the compounds were added prior to inoculation. For the “during” condition, no significant effect was seen for moxidectin and a significant, albeit limited, effect was observed for ivermectin. A strong reduction in viral titer was seen when the compounds were added at 2 hpi (Fig. 2C). For moxidectin, the infectious virus titer was reduced to  $1.5 \pm 1.0 \times 10^3$  PFU/ml, corresponding to a reduction of 98.6%, and for ivermectin, the titer was reduced to  $1.5 \pm 0.8 \times 10^2$  (99.9% reduction) compared to the corresponding EtOH control. No significant effect was seen when moxidectin or ivermectin was added at 4 or 6 hpi compared to the EtOH control (see Fig. S2). Collectively, these results indicate that both moxidectin and ivermectin directly interfere with the viral infectious replication cycle in cells. This shows that either the compounds act at the early stages of RNA replication/translation (within 2 to 4 h postinfection) or that the compounds interfere with late stages of virus assembly/secretion (i.e., need to be present for more than 4 h to exert their antiviral effect).

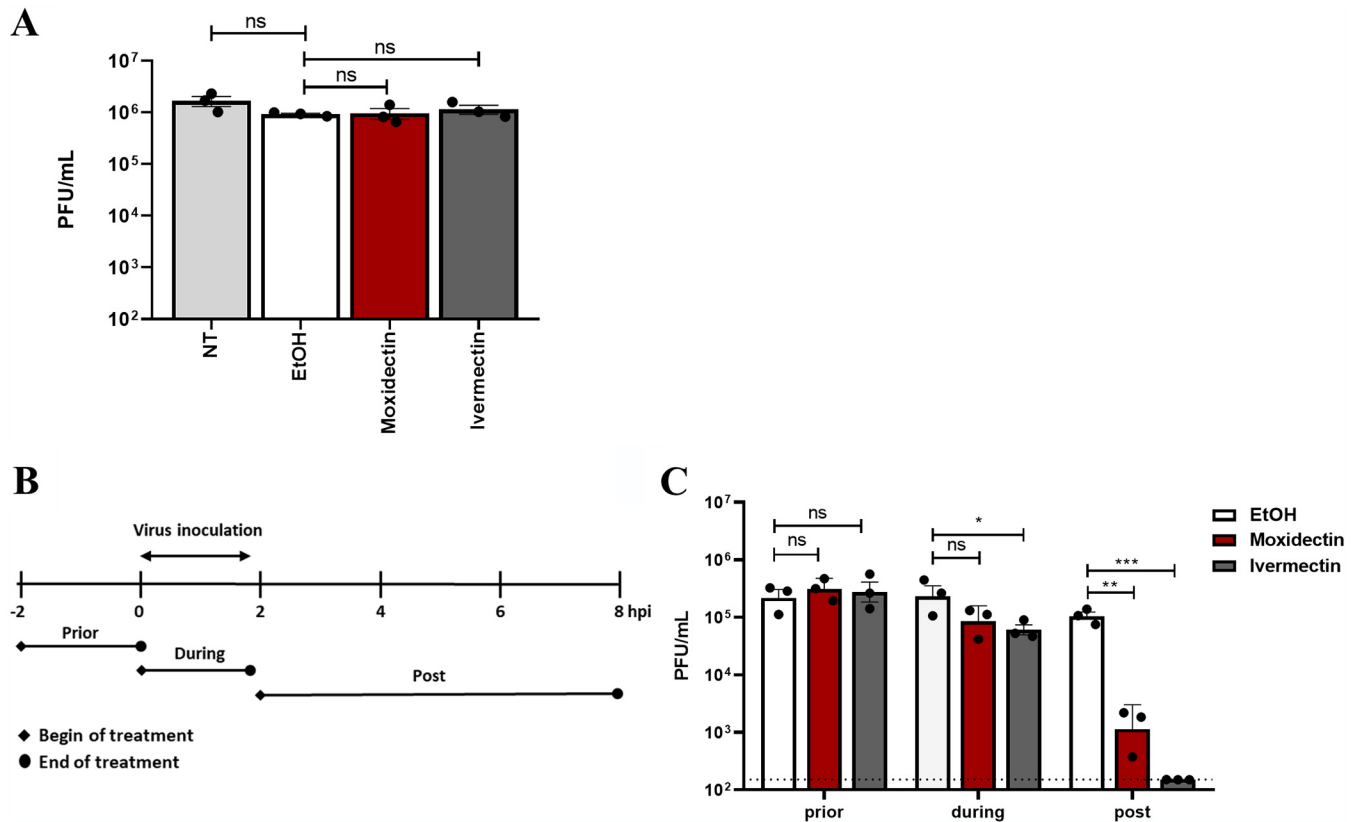


**FIG 2** Moxidectin and ivermectin predominantly inhibit SARS-CoV-2 under postinfection conditions. (A) Virucidal effect of moxidectin and ivermectin on SARS-CoV-2. (B) Schematic summary of the time-of-drug-addition experiment. (C) Vero E6 cells were infected with SARS-CoV-2 at MOI 1 for 2 h, after which the inoculum was removed. Cells were treated with moxidectin or ivermectin at a concentration of  $10 \mu\text{M}$ , or with the corresponding volume of EtOH, as depicted in panel B. At 8 hpi, cell supernatants were harvested, and the virus titer was determined via plaque assay. Dotted lines indicate the detection limit of plaque assay. Each dot represents data from a single independent experiment. Data for the three independent experiments are presented as mean  $\pm$  SEM. Statistical analysis was carried out by comparing treated samples with the EtOH control using a Student's *t* test. \*\*\* ( $P < 0.001$ ), \*\* ( $P < 0.01$ ), \* ( $P < 0.05$ ), and "ns" (nonsignificant).

### Moxidectin and ivermectin do not exhibit anti- SARS-CoV-2 activity in Calu-3 and primary human bronchial epithelial cells.

We next sought to validate the antiviral potential of moxidectin and ivermectin in human lung epithelial Calu-3 cells, which have previously been shown to support SARS-CoV-2 replication (37). Prior to infectivity assays, the cellular cytotoxicity of both compounds at 5 and  $10 \mu\text{M}$  was determined using the MTS assay. At these concentrations, no cytotoxicity was observed (see Fig. S3). Accordingly, we proceeded by infecting Calu-3 cells with SARS-CoV-2 at MOI 1 in the presence or absence of  $5 \mu\text{M}$  and  $10 \mu\text{M}$  moxidectin or ivermectin. In the absence of the drugs (NT condition), infection led to a release of an average  $1.5 \pm 2.3 \times 10^4$  PFU/ml at 8 hpi (Fig. 3A). A comparable titer was observed for the EtOH control ( $1.7 \pm 2.5 \times 10^4$  PFU/ml). A mild to moderate reduction in viral titers was observed in the presence of moxidectin and ivermectin, but this was found to be not statistically significant.

Because the human respiratory tract represents the primary site of virus infection (38), we decided to further verify the antiviral activity of moxidectin and ivermectin in a human-based cell system. Here, we used PBECs cultured under ALI culture system. Cells grown under ALI conditions undergo cellular differentiation, thus mimicking crucial physiological properties similar to those found *in vivo* (39–41). Prior to performing the antiviral assays in this model system, we first assessed the cytotoxicity of  $10 \mu\text{M}$  moxidectin and ivermectin at 48 h of treatment, using live-death staining and a LDH release assay. Both assays showed a viability above 90% compared to the EtOH control (see Fig. S4) ALI-cultured PBECs were incubated with  $10 \mu\text{M}$  moxidectin or ivermectin at the basolateral side and infected with SARS-CoV-2 at MOI 5 at the apical side, as

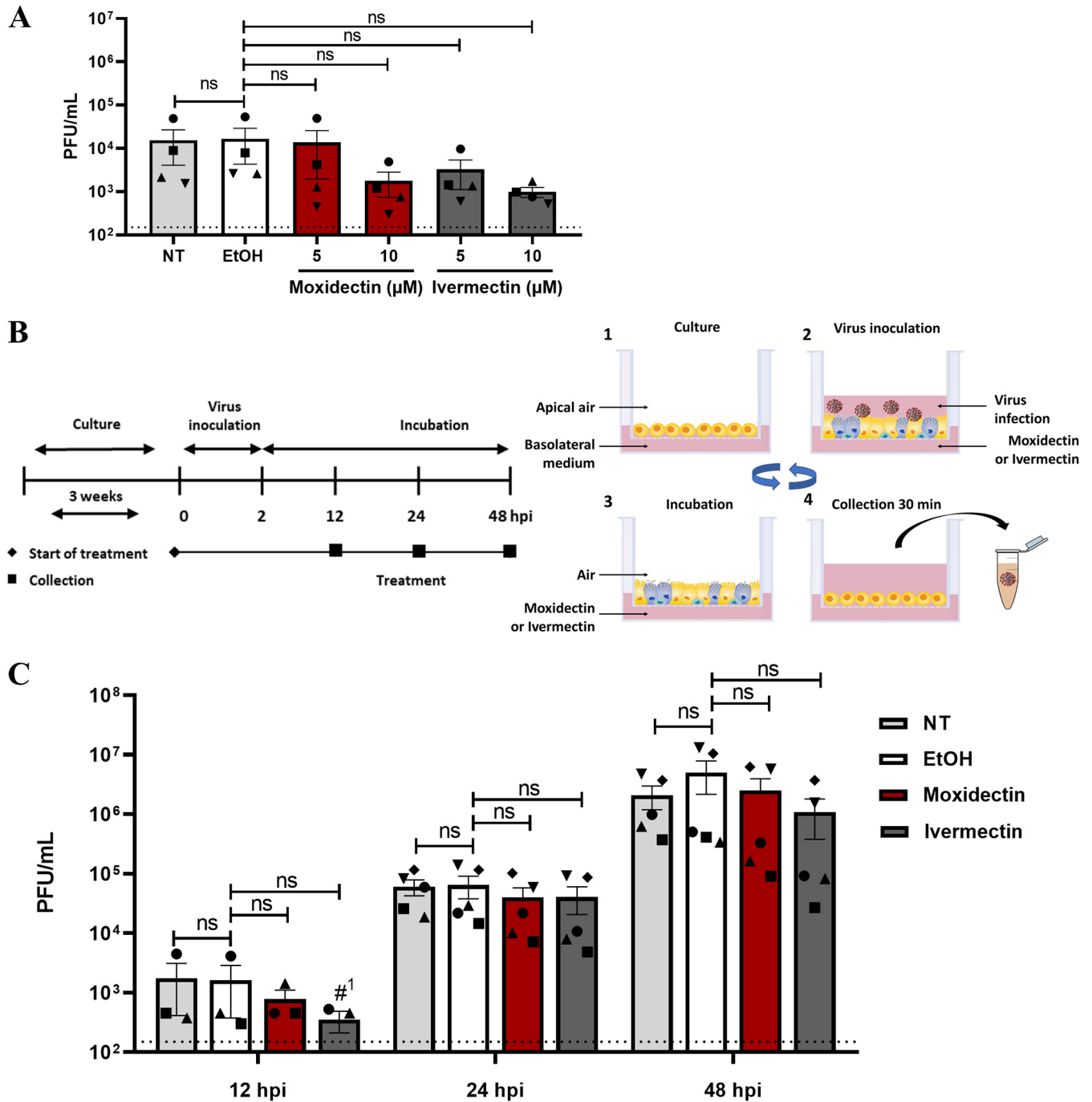


**FIG 3** Moxidectin and ivermectin have no significant effect on SARS-CoV-2 infection in human-derived cell models. (A) Calu-3 cells were treated with 5 and 10  $\mu\text{M}$  moxidectin or ivermectin, or the highest respective concentration of EtOH, in the presence of SARS-CoV-2 at MOI 1. At 8 hpi, cell supernatants were harvested, and the number of infectious virus particles produced was determined by plaque assay. Each dot represents data from a single independent experiment. (B) Schematic representation of the experimental design. (1) PBECs were cultured on permeable inserts under ALI conditions for  $\sim 3$  weeks. (2) Cells were inoculated with SARS-CoV-2 MOI 5 at the apical side of the insert, and treated with 10  $\mu\text{M}$  moxidectin, ivermectin, or the corresponding volume of EtOH at the basolateral side until the collection time, as shown in the schematics (3) Following virus inoculation, virus was removed by washing with media, and the cells were left under ALI conditions until virus collection. (4) For the final collection, cells were incubated with medium for 30 min, and the progeny virus produced was collected. After collection, cells were exposed to air again (3) until the next collection time point, and steps 3 and 4 were repeated until the end of treatment. (C) The antiviral activity of moxidectin and ivermectin in PBECs. Dotted lines indicate the threshold of detection. Scheme adapted from Stemcell Technologies (67). Each dot represents data from a single independent experiment. The number of values below the detection limit are indicated #x. Data from the five different donors are presented as mean  $\pm$  SEM. A Student's *t* test was used to evaluate statistical differences and a *P* value of  $\leq 0.05$  was considered significant. \* ( $P \leq 0.05$ ), \*\* ( $P \leq 0.01$ ), \*\*\* ( $P \leq 0.001$ ), and "ns" (nonsignificant).

indicated in the schematics (Fig. 3B). Supernatants were harvested from the apical side at 12, 24, and 48 hpi and titers were determined using plaque assays. Importantly, despite the strong antiviral effect in Vero E6 cells, no significant antiviral activity was seen in the apical washes of moxidectin- or ivermectin-treated PBECs when compared to the EtOH control at all time points tested (Fig. 3C). Next to moxidectin and ivermectin, we also tested the antiviral activity of resveratrol in the same donors and observed a potent antiviral effect in this model system, thereby confirming the validity of the experimental settings (42).

## DISCUSSION

We confirm the previously published antiviral activity of ivermectin (18) in Vero E6 cells and showed an antiviral effect of moxidectin against SARS-CoV-2 in these cells. Further in-depth mode-of-action experiments revealed that moxidectin and ivermectin actively interfere with virus replication. Unfortunately, despite the promising antiviral properties of moxidectin and ivermectin in Vero E6 cells, the drugs did not show any antiviral activity in human airway-derived cell models. Collectively, the data show that the potency of moxidectin and ivermectin are species- or cell-type- specific and provide an explanation for the discordant findings in literature, where positive effects were found in Vero cells, but no clinically relevant patient outcomes could be demonstrated in human studies.

To demonstrate which steps of the SARS-CoV-2 replication cycle are affected by moxidectin or ivermectin in Vero E6 cells, we performed time-of-drug-addition experiments. The strongest effect was seen when either moxidectin or ivermectin was added after the onset of infection, suggesting that the compounds do not interfere with processes related to viral entry, such as virus-cell binding, internalization, or membrane fusion. We hypothesize that the compounds either directly interfere with early stages of RNA translation/replication or indirectly at late stages of the virus replication cycle (due to prolonged incubation). Other studies revealed that ivermectin blocks replication of HIV-1 and DENV viruses (13, 14) by binding and inhibiting cellular importin (IMP)  $\alpha/\beta$ -mediated transport of viral proteins to the nucleus (13, 43). Ivermectin has also been shown to inhibit NS3 helicase activity, thereby inhibiting flavivirus replication (44). Our findings hint toward a mechanism in which both drugs restrict SARS-CoV-2 replication by modulating cellular factors or processes which control replication in Vero E6 cells but are absent in human-derived Calu-3 and PBECs.

Currently (as of April 29, 2021), 65 clinical trials are registered to evaluate the efficacy of ivermectin as a prophylactic or therapeutic drug, and 21 of these have been completed (25). Many of these trials have serious limitations, such as small sample size, lack of blinding, and lack of pre-registration for some trials, and they therefore carry a risk of bias (26, 28, 45–51). Apart from the problem of bias, only five trials have directly compared ivermectin with standard of care and reported clinically crucial outcomes such as mortality (27, 29, 52–54). The WHO recently stated: “The current evidence of effect of ivermectin on mortality, mechanical ventilation, hospital admission and duration of hospitalization remains uncertain.” (28) Yet many clinical trials are still ongoing. The observed lack of antiviral activity of ivermectin in the biologically relevant PBECs model reported here, together with the poor pharmacological properties of ivermectin (21, 23, 24), do not forecast success for ongoing clinical trials on its usage in COVID-19 patients.

SARS-CoV-2 can also infect several economically important livestock, such as cats, dogs, minks, lions, and tigers (55–60). Inhibition of virus replication in these animals could thus offer an effective strategy for controlling virus dissemination. Both drugs inhibited SARS-CoV-2 infection in African green monkey-derived kidney epithelial (Vero E6) cells. Since both compounds have already been FDA approved for use in animals (61, 62), our results in Vero E6 warrant follow-up studies in relevant animal cell systems to assess their potential as antivirals for economically important livestock.

In conclusion, we elucidated that while both moxidectin and ivermectin exhibit

antiviral activity in Vero E6, they do not reduce SARS-CoV-2 replication in human-airway-derived cell models. While immortalized cell lines such as Vero E6 may be useful in a primary screening of inhibitors, it is important to determine true relevance of the inhibitors in a biological relevant model. In humans, the airway epithelium is the main target for SARS-CoV-2 (34, 63), and therefore PBECs grown under ALI conditions, but not Vero cells, mimic crucial physiological properties similar to those found *in vivo* (39 to 41). We therefore advocate for more rigorous antiviral drug testing in relevant systems prior to evaluating their efficacy in clinical trials.

## MATERIALS AND METHODS

**Chemicals and reagents.** Ivermectin (Sigma-Aldrich, MO, USA) and moxidectin (European Pharmacopeia reference standard, Strasbourg, France) were dissolved in absolute ethanol (EtOH; Sigma-Aldrich, MO, USA) to a final concentration of 5 mM and stored at  $-20^{\circ}\text{C}$ . The maximum final EtOH concentration corresponded to 0.2% in all experiments.

**Virus stock and titration.** SARS-CoV-2 strain/NL/2020 (European Virus archive global [EVAg], 010V-03903) was produced in Vero E6 cells. The cells were infected at a multiplicity of infection (MOI) of 1, and 48 h postinfection (hpi), supernatants containing progeny virions were harvested, centrifuged, aliquoted, and stored at  $-80^{\circ}\text{C}$ . The obtained virus was passaged twice prior to usage in the experiments described in this manuscript. At these passaging conditions, no cell culture adaptations were observed, as the sequence of the subsequent P3 virus stock (for a parallel project) was still identical to the original strain. The infectious virus titer was determined by a plaque assay on Vero E6 cells. Briefly, Vero E6 cells were infected for 2 h with 10-fold serial dilutions of samples, after which cells were overlaid with a 1:1 mixture of 2% agarose (Lonza; Basel, Switzerland) and 2X MEM medium. At 72 hpi, the plaques were fixed using 10% formaldehyde (Alfa Aesar; Kandel, Germany) and stained using crystal violet (Sigma-Aldrich; MO, USA). Infectious titers are stated as PFU per ml. One plaque in 10-fold dilution corresponds to 150 PFU/ml and was set as the threshold of detection for all experiments.

**Cell culture.** The African green monkey Vero E6 cell line (ATCC CRL-1586), kindly provided by Gorben Pijlman (Wageningen University, Wageningen, the Netherlands), was maintained in Dulbecco's minimal essential medium (DMEM) (Gibco, Paiskey, UK), high glucose supplemented with 10% fetal bovine serum (FBS; Lonza, Basel, Switzerland), penicillin (100 U/ml), and streptomycin (100 U/ml; Gibco, Paiskey, UK). The human lung epithelial cell line Calu-3 (ATCC HTB-55) was maintained in DMEM F-12 (Lonza, Basel, Switzerland) supplemented with 10% FBS, 1% Glutamax (Thermo Fisher Scientific Inc., Waltham, MA, USA), 1% non-essential amino acid (Thermo Fisher Scientific Inc., Waltham, MA, USA), penicillin (100 U/ml), and streptomycin (100 U/ml). All cells were mycoplasma-negative and maintained at  $37^{\circ}\text{C}$  under 5%  $\text{CO}_2$ . Primary human bronchial epithelial cells (PBECs) were cultured from bronchial brushing obtained by fiberoptic bronchoscopy, performed using a standardized protocol during conscious sedation (64, 65). The medical ethics committee of the University Medical Center Groningen approved the study (METC 2019/338), and all subjects gave their written informed consent. The donors were 3 male and 2 female nonsmoking, healthy control volunteers, with normal lung function ( $\text{FEV}_1/\text{FVC} > 70\%$ ,  $\text{FEV}_1 > 90\%$  predicted) and an absence of bronchial hyperresponsiveness to methacholine ( $\text{PC}_{20}$  methacholine  $> 8$  mg/ml). PBECs were cultured and fully differentiated under ALI conditions, in Transwell inserts, as previously described (66).

**Cytotoxicity assays. (i) MTS assay.** An MTS assay to determine cytotoxicity was performed using the CellTiter 96 AQueous One Solution Cell Proliferation assay kit, using the manufacturer's instructions from Promega (Madison, WI, USA). Vero E6 cells were seeded in 96-well plates at a density of 10,000 cells/well. The following day, cells were treated with either increasing concentrations of moxidectin or ivermectin (ranging from 0 to 80  $\mu\text{M}$ ) for 8 h, or both compounds at 10  $\mu\text{M}$  for 60 h, along with an equivalent volume of EtOH. Thereafter, 20  $\mu\text{l}$  of the MTS/PMS reagent was added to each well and the cells were further incubated at  $37^{\circ}\text{C}$  for 2 h. Subsequently, 10% SDS solution was added to stop the reaction and the absorbance was measured at 490 nm using a microplate reader (BioTek, Winnooski, VT). Calu-3 cells were seeded in a 96-well plate at a density of 40,000 cells/well. Cells were treated with 5 and 10  $\mu\text{M}$  moxidectin, ivermectin, or an equivalent volume of EtOH for 8 h. The same steps were followed as described above for Vero E6 cells. Cytotoxicity was determined based on the following formula:

$$\% \text{ cytotoxicity} = \frac{(\text{absorbance sample} - \text{absorbance blank})}{(\text{absorbance negative control} - \text{absorbance blank})} \times 100$$

**(ii) LDH cytotoxicity assay.** An LDH assay was performed using the CyQUANT<sup>TM</sup> LDH Cytotoxicity assay kit (Thermo Fisher Scientific, Inc., Waltham, MA, USA). PBECs cultured under ALI conditions were treated with 10  $\mu\text{M}$  moxidectin, ivermectin, or an equivalent volume of EtOH at the basolateral side for 48 h at  $37^{\circ}\text{C}$ . Thereafter, LDH release was determined at the apical side. Here, 200  $\mu\text{l}$  of Opti-MEM (Gibco, Paiskey, UK) was added to the apical side 30 min prior to the harvest. The apical harvest was clarified by centrifuging at  $2000 \times g$  at  $4^{\circ}\text{C}$ . Levels of LDH were determined in all experimental conditions according to the manufacturer's instructions. The absorbance was measured at 490 and 680 nm using a microplate reader (BioTek, Winnooski, VT). The absorbance at 680 nm was subtracted from the absorbance at 490 nm and cytotoxicity was calculated as described below:



$$\% \text{ cytotoxicity} = \frac{(\text{compound-treated LDH activity} - \text{spontaneous LDH activity})}{(\text{maximum LDH activity} - \text{spontaneous LDH activity})} \times 100$$

**Live/dead staining and flow cytometry.** PBECs cultured under ALI conditions were treated with 10  $\mu\text{M}$  moxidectin, ivermectin, or an equivalent volume of EtOH at the basolateral side for 48 h at 37°C. Subsequently, cells were harvested by trypsinization and stained with fixable viability dye eFluor780 (Thermo Fisher Scientific) for 20 min at 4°C. Next, cells were washed with fluorescence-activated cell sorter (FACS) buffer (1X phosphate-buffered saline, 2% FBS, 1% EDTA), centrifuged, and fixed with 4% paraformaldehyde for 10 min at 4°C. After fixation, cells were washed, centrifuged, and resuspended in FACS buffer. Flow cytometry analyses were performed using the LSR-2 flow cytometer (BD Biosciences, San Jose, CA, USA) and data was further analyzed using Kaluza analysis software, version 2.1 (Beckman Coulter, Fullerton, CA, USA).

**Antiviral assays in Vero E6 and Calu-3.** Vero E6 cells were seeded at a density of  $1.3 \times 10^5$  cells/well in 12-well plates. The next day, the medium was replaced with 0.25 ml of DMEM (2% FBS) containing the virus inoculum (MOI 1), in the presence of either increasing concentrations of compounds or the equivalent volume of EtOH. Following 2 h adsorption at 37°C, the virus inoculum was removed, after which the cells were washed twice and fresh DMEM (10% FBS) containing either the compounds or EtOH was added. At 8 hpi, cell supernatants were harvested and titrated using plaque assays. For the durability assay, Vero E6 cells were infected with SARS-CoV-2 at MOI 0.01 and treated with 10  $\mu\text{M}$  moxidectin, ivermectin, or the equivalent volume of EtOH. Supernatants were collected at 16, 24, 40, and 60 hpi. A lower MOI was used to allow multiple rounds of infection. Samples were titrated using plaque assays. Calu-3 cells were seeded at a density of  $2 \times 10^5$  cells/well in 24-well plates. At 48 h post-seeding, infection was performed in 0.2 ml of DMEM (2% FBS) containing virus inoculum (MOI 1) and 5 or 10  $\mu\text{M}$  moxidectin, ivermectin, or the corresponding volume of EtOH. Cell supernatants were harvested at 8 hpi and titrated using plaque assays.

**Antiviral assays in primary bronchial epithelial cells.** Following 3 weeks of ALI culture, human primary bronchial epithelial cells (PBECs) were washed twice with Opti-MEM to remove excess mucus. At the time of infection, 10  $\mu\text{M}$  moxidectin, ivermectin, or the equivalent volume of EtOH was added at the basolateral side of the insert (12-well). The apical side was inoculated with SARS-CoV-2 at MOI 5. At 2 hpi, cells were washed twice with Opti-MEM and left on air at 37°C until collection. Thirty minutes prior to collection (12, 24, and 48 hpi), 150  $\mu\text{l}$  of Opti-MEM was added to the apical side of the ALI cultures, and virus was harvested by incubating for 30 min at 37°C. Infectious virus titers were determined using plaque assays.

**Virucidal assays.** SARS-CoV-2 particles ( $2.5 \times 10^5$  PFU) were incubated in the presence or absence of 10  $\mu\text{M}$  moxidectin, ivermectin, or the equivalent volume of EtOH for 2 h at 37°C in 300  $\mu\text{l}$  of DMEM (2% FBS). Infectious virus titers were determined using plaque assays.

**Time-of-drug-addition assays.** For the time-of-drug-addition experiments, Vero E6 cells were treated with 10  $\mu\text{M}$  moxidectin, ivermectin, or the corresponding volume of EtOH at three time periods: prior to, during, or post-inoculation (Fig. 2B). For the “pre-treatment” condition, cells were incubated with the compounds for 2 h prior to infection. At the time of infection, cells were washed three times and infected with SARS-CoV-2 at MOI 1 for 2 h. At 2 hpi, cells were washed three times with plain DMEM, medium was replaced with DMEM 10% FBS, and incubation was continued until collection. For the “during” condition, the compounds were present together with the virus inoculum only during the 2 h infection time. For the postinoculation condition, the compounds were added to the cell culture medium at 2, 4, and 6 h postinoculation. All supernatants were collected at 8 hpi, clarified by centrifugation, and used to quantify the infectious particle titers using plaque assays.

**Statistical analysis.** The concentrations at which moxidectin and ivermectin reduced virus particle production by 50% and 90% are referred to as EC50 and EC90, respectively. Dose-response curves were fitted by non-linear regression analysis employing a sigmoidal model. All data were analyzed in GraphPad Prism software (La Jolla, CA, USA). Data are presented as mean  $\pm$  SEM. A Student's *t* test was used to evaluate statistical differences between treated samples, and a *P* value  $\leq$  0.05 was considered significant, with \* *P*  $\leq$  0.05, \*\* *P*  $\leq$  0.01, \*\*\* *P*  $\leq$  0.001, and “ns” considered nonsignificant.

## SUPPLEMENTAL MATERIAL

Supplemental material is available online only.

**SUPPLEMENTAL FILE 1**, PDF file, 0.6 MB.

## ACKNOWLEDGMENTS

Grant support was provided by the University Medical Center of Groningen and Marie Skłodowska-Curie Cofund grant under the European Union's Horizon 2020 Research and Innovation Program PRONKJEWAIL (713660). The funders had no role in study design, data collection and interpretation, or the decision to submit the work for publication.

We thank Y. Bhide for help in the design of experiments.

Author contributions. N.D.K., B.M.t.E., E.M.B., M.C.N., Y.S., I.A.R.-Z. and J.M.S. designed the experiments. N.D.K., B.M.t.E., E.M.B., B.T., D.P.l.v.d.P., H.H.v.d.E.-M., D.v.G., and L.A. executed the experiments. O.A.C. and M.v.d.B. selected, recruited, and sampled donors. N.D.K., E.M.B. I.A.R.-Z. and J.M.S. wrote the manuscript. All authors edited the manuscript.

## REFERENCES

- Zhou P, Yang XL, Wang XG, Hu B, Zhang L, Zhang W, Si HR, Zhu Y, Li B, Huang CL, Chen HD, Chen J, Luo Y, Guo H, Jiang RD, Liu MQ, Chen Y, Shen XR, Wang X, Zheng XS, Zhao K, Chen QJ, Deng F, Liu LL, Yan B, Zhan FX, Wang YY, Xiao GF, Shi ZL. 2020. A pneumonia outbreak associated with a new coronavirus of probable bat origin. *Nature* 579:270–273. <https://doi.org/10.1038/s41586-020-2012-7>.
- Sohrabi C, Alsafi Z, O'Neill N, Khan M, Kerwan A, Al-Jabir A, Iosifidis C, Agha R. 2020. World Health Organization declares global emergency: a review of the 2019 novel coronavirus (COVID-19). *Int J Surg* 76:71–76. <https://doi.org/10.1016/j.ijssu.2020.02.034>.
- WHO. 2021. Coronavirus disease (COVID-19) pandemic. <https://covid19.who.int/>. Accessed 29 April 2021.
- Chan W, He B, Wang X, He M-L. 2020. Pandemic COVID-19: current status and challenges of antiviral therapies. *Genes Dis* 7:502–519. <https://doi.org/10.1016/j.gendis.2020.07.001>.
- Zhang J, Xie B, Hashimoto K. 2020. Current status of potential therapeutic candidates for the COVID-19 crisis. *Brain Behav Immun* 87:59–73. <https://doi.org/10.1016/j.bbi.2020.04.046>.
- Pan H, Peto R, Henao-Restrepo A-M, Preziosi M-P, Sathiyamoorthy V, Abdool Karim Q, Alejandria MM, Hernández García C, Kiemy M-P, Malekzadeh R, Murthy S, Reddy KS, Roses Periago M, Abi Hanna P, Ader F, Al-Bader AM, Alhasawi A, Allum E, Alotaibi A, Alvarez-Moreno CA, Appadoo S, Asiri A, Aukrust P, Barratt-Due A, Bellani S, Branca M, Cappel-Porter HBC, Cerrato N, Chow TS, Como N, Eustace J, García PJ, Godbole S, Gotuzzo E, Grisevicius L, Hamra R, Hassan M, Hassany M, Hutton D, Irmansyah I, Jancoriene L, Kirwan J, Kumar S, Lennon P, Lopardo G, Lydon P, Magrini N, Maguire T, Manevska S, Manuel O, WHO Solidarity Trial Consortium, et al. 2021. Repurposed antiviral drugs for COVID-19 – interim WHO solidarity trial results. *N Engl J Med* 384:497–511. <https://doi.org/10.1056/NEJMoa2023184>.
- Rochewerg B, Agarwal A, Siemieniuk RA, Agoritsas T, Lamontagne F, Askie L, Lytvyn L, Leo Y-S, Macdonald H, Zeng L, Amin W, Burhan E, Bausch FJ, Alcafee CS, Cecconi M, Chanda D, Du B, Geduld H, Gee P, Harley N, Hashimi M, Hunt B, Kabra SK, Kanda S, Kawano-Dourado L, Kim Y-J, Kissoon N, Kwizera A, Mahaka I, Manai H, Mino G, Nsutebu E, Preller J, Pshenichnaya N, Qadir N, Sabzwari S, Sarin R, Shankar-Hari M, Sharland M, Shen Y, Ranganathan SS, Souza JP, Stegemann M, De Sutter A, Ugarte S, Venkatapuram S, Dat VQ, Vuyiseka D, Wijewickrama A, Maguire B, et al. 2020. A living WHO guideline on drugs for COVID-19. *BMJ* 370:m3379. <https://doi.org/10.1136/bmj.m3379>.
- NIH. 2021. Therapeutic management of adults with COVID-19. <https://www.covid19treatmentguidelines.nih.gov/therapeutic-management/>. Accessed 29 April, 2021.
- Prichard R, Menez C, Lespine A. 2012. Moxidectin and the avermectins: consanguinity but not identity. *Int J Parasitol Drugs Drug Resist* 2: 134–153. <https://doi.org/10.1016/j.ijpddr.2012.04.001>.
- EMA. 2017. Moxidectin-containing veterinary medicines used in cattle, sheep and horses <https://www.ema.europa.eu/en/medicines/veterinary/referrals/moxidectin-containing-veterinary-medicines-used-cattle-sheep-horses>. Accessed 24 February, 2021.
- EMA. 2009. Ivermectin. <https://www.ema.europa.eu/en/medicines/veterinary/referrals/ivermectin>. Accessed 24 February 2021.
- Makhani L, Khatib A, Corbeil A, Kariyawasam R, Raheel H, Clarke S, Challa P, Hagopian E, Chakrabarti S, Schwartz KL, Boggild AK. 2019. 2018 in review: five hot topics in tropical medicine. *Trop Dis Travel Med Vaccines* 5:5. <https://doi.org/10.1186/s40794-019-0082-z>.
- Wagstaff KM, Sivakumaran H, Heaton SM, Harrich D, Jans DA. 2012. Ivermectin is a specific inhibitor of importin alpha/beta-mediated nuclear import able to inhibit replication of HIV-1 and dengue virus. *Biochem J* 443:851–856. <https://doi.org/10.1042/BJ20120150>.
- Tay MY, Fraser JE, Chan WK, Moreland NJ, Rathore AP, Wang C, Vasudevan SG, Jans DA. 2013. Nuclear localization of dengue virus (DENV) 1–4 nonstructural protein 5; protection against all 4 DENV serotypes by the inhibitor Ivermectin. *Antiviral Res* 99:301–306. <https://doi.org/10.1016/j.antiviral.2013.06.002>.
- Lundberg L, Pinkham C, Baer A, Amaya M, Narayanan A, Wagstaff KM, Jans DA, Kehn-Hall K. 2013. Nuclear import and export inhibitors alter capsid protein distribution in mammalian cells and reduce Venezuelan Equine Encephalitis Virus replication. *Antiviral Res* 100:662–672. <https://doi.org/10.1016/j.antiviral.2013.10.004>.
- Gotz V, Magar L, Dornfeld D, Giese S, Pohlmann A, Hoper D, Kong BW, Jans DA, Beer M, Haller O, Schwemmler M. 2016. Influenza A viruses escape from MxA restriction at the expense of efficient nuclear vRNP import. *Sci Rep* 6:23138. <https://doi.org/10.1038/srep25428>.
- Varghese BS, Kaukinen P, Glasker S, Bespalov M, Hanski L, Wennerberg K, Kummerer FM, Ahola T. 2016. Discovery of berberine, abamectin and ivermectin as antivirals against chikungunya and other alphaviruses. *Antiviral Res* 126:117–124. <https://doi.org/10.1016/j.antiviral.2015.12.012>.
- Caly L, Druce JD, Catton MG, Jans DA, Wagstaff KM. 2020. The FDA-approved drug ivermectin inhibits the replication of SARS-CoV-2 in vitro. *Antiviral Res* 178:104787. <https://doi.org/10.1016/j.antiviral.2020.104787>.
- Ketkar H, Yang L, Wormser GP, Wang P. 2019. Lack of efficacy of ivermectin for prevention of a lethal Zika virus infection in a murine system. *Diagn Microbiol Infect Dis* 95:38–40. <https://doi.org/10.1016/j.diagmicrobio.2019.03.012>.
- Yamasmith E, Avirutnan P, Mairiang D, Tanrumluk S, Suputtamongkol Y, A-Hamad Saleh-Ariong F, Angkasekwinai N, Wongsawa E, Fongsri U. 2018. Efficacy and safety of ivermectin against dengue infection: a phase III, randomized, double-blind, placebo-controlled trial, p In (ed), *Internal Medicine and One Health*, Chonburi
- Momekov G, Momekova D. 2020. Ivermectin as a potential COVID-19 treatment from the pharmacokinetic point of view: antiviral levels are not likely attainable with known dosing regimens. *Biotechnol Biotechnol Equip* 34:469–474. <https://doi.org/10.1080/13102818.2020.1775118>.
- Bray M, Rayner C, Noel F, Jans D, Wagstaff K. 2020. Ivermectin and COVID-19: a report in antiviral research, widespread interest, an FDA warning, two letters to the editor and the authors' responses. *Antiviral Res* 178: 104805. <https://doi.org/10.1016/j.antiviral.2020.104805>.
- Schmith VD, Zhou JJ, Lohmer LRL. 2020. The approved dose of ivermectin alone is not the ideal dose for the treatment of COVID-19. *Clin Pharmacol Ther* 108:762–765. <https://doi.org/10.1002/cpt.1889>.
- Pena-Silva R, Duffull SB, Steer AC, Jaramillo-Rincon SX, Gwee A, Zhu X. 2021. Pharmacokinetic considerations on the repurposing of ivermectin for treatment of COVID-19. *Br J Clin Pharmacol* 87:1589–1590. <https://doi.org/10.1111/bcp.14476>.
- clinicaltrials.gov. 2021. Ivermectin and COVID-19. <https://clinicaltrials.gov/ct2/results?recrs=&cond=covid-19&term=ivermectin+and+covid-19&cntry=&state=&city=&dist=>. Accessed 29 April, 2021.
- Chaccour C, Casellas A, Blanco-Di Matteo A, Pineda I, Fernandez-Montero A, Ruiz-Castillo P, Richardson MA, Rodriguez-Mateos M, Jordan-Iborra C, Brew J, Carmona-Torre F, Giraldez M, Laso E, Gabaldon-Figueira JC, Dobano C, Moncunill G, Yuste JR, Del Pozo JL, Rabinovich NR, Schoning V, Hammann F, Reina G, Sadaba B, Fernandez-Alonso M. 2021. The effect of early treatment with ivermectin on viral load, symptoms and humoral response in patients with non-severe COVID-19: A pilot, double-blind, placebo-controlled, randomized clinical trial. *EClinicalMedicine* 32: 100720. <https://doi.org/10.1016/j.eclinm.2020.100720>.
- Lopez-Medina E, Lopez P, Hurtado IC, Davalos DM, Ramirez O, Martinez E, Diazgranados JA, Onate JM, Chavarriaga H, Herrera S, Parra B, Liberos E, Jaramillo R, Avendano AC, Toro DF, Torres M, Lesmes MC, Rios CA, Caicedo I. 2021. Effect of ivermectin on time to resolution of symptoms among adults with mild COVID-19: a randomized clinical trial. *JAMA* 325: 1426–1435. <https://doi.org/10.1001/jama.2021.3071>.
- WHO. 2021. Therapeutics and COVID-19: living guidelines. <https://www.who.int/publications/i/item/WHO-2019-nCoV-therapeutics-2021.1>. Accessed 29 April, 2021.
- Gonzalez JLB, Gámez MG, Enciso EAM, Maldonado RJE, Palacios DH, Campos SD, Robles IO, Guzmán MJM, Díaz ALG, Peña CMG, Medina LM, Colin VAM, Manuel AGJ. 2021. Efficacy and safety of ivermectin and hydroxychloroquine in patients with severe COVID-19. A randomized controlled trial. *medRxiv Preprint* <https://doi.org/10.1101/2021.02.18.21252037>.
- Cobb R, Boeckh A. 2009. Moxidectin: a review of chemistry, pharmacokinetics and use in horses. *Parasit Vectors* 2 Suppl 2:S5. <https://doi.org/10.1186/1756-3305-2-S2-S5>.
- Prichard RK, Geary TG. 2019. Perspectives on the utility of moxidectin for the control of parasitic nematodes in the face of developing anthelmintic resistance. *Int J Parasitol Drugs Drug Resist* 10:69–83. <https://doi.org/10.1016/j.ijpddr.2019.06.002>.
- Milton P, Hamley JID, Walker M, Basanez MG. 2020. Moxidectin: an oral treatment for human onchocerciasis. *Expert Rev Anti Infect Ther* <https://doi.org/10.1080/14787210.2020.1792772>:1–15.
- Opoku NO, Bakajika DK, Kanza EM, Howard H, Mambandu GL, Nyathirombo A, Nigo MM, Kasonia K, Masembe SL, Mumbere M, Kataliko K, Larbelee JP, Kpawor M, Bolay KM, Bolay F, Asare S, Attah SK, Oliphon G, Vaillant M, Halleux CM, Kuesel AC. 2018. Single dose moxidectin versus

- ivermectin for *Onchocerca volvulus* infection in Ghana, Liberia, and the Democratic Republic of the Congo: a randomized, controlled, double-blind phase 3 trial. *Lancet* 392:1207–1216. [https://doi.org/10.1016/S0140-6736\(17\)32844-1](https://doi.org/10.1016/S0140-6736(17)32844-1).
34. Leist SR, Schafer A, Martinez DR. 2020. Cell and animal models of SARS-CoV-2 pathogenesis and immunity. *Dis Model Mech* 13. <https://doi.org/10.1242/dmm.046581>.
  35. Matsuyama S, Nao N, Shirato K, Kawase M, Saito S, Takayama I, Nagata N, Sekizuka T, Katoh H, Kato F, Sakata M, Tahara M, Kutsuna S, Ohmagari N, Kuroda M, Suzuki T, Kageyama T, Takeda M. 2020. Enhanced isolation of SARS-CoV-2 by TMPRSS2-expressing cells. *Proc Natl Acad Sci U S A* 117:7001–7003. <https://doi.org/10.1073/pnas.2002589117>.
  36. Ogando NS, Dalebout TJ, Zevenhoven-Dobbe JC, Limpens R, van der Meer Y, Caly L, Druce J, de Vries JJC, Kikkert M, Barcena M, Sidorov I, Snijder EJ. 2020. SARS-coronavirus-2 replication in Vero E6 cells: replication kinetics, rapid adaptation and cytopathology. *J Gen Virol* 101:925–940. <https://doi.org/10.1099/jgv.0.001453>.
  37. Chu H, Chan JF, Yuen TT, Shuai H, Yuan S, Wang Y, Hu B, Yip CC, Tsang JO, Huang X, Chai Y, Yang D, Hou Y, Chik KK, Zhang X, Fung AY, Tsoi HW, Cai JP, Chan WM, Ip JD, Chu AW, Zhou J, Lung DC, Kok KH, To KK, Tsang OT, Chan KH, Yuen KY. 2020. Comparative tropism, replication kinetics, and cell damage profiling of SARS-CoV-2 and SARS-CoV with implications for clinical manifestations, transmissibility, and laboratory studies of COVID-19: an observational study. *Lancet Microbe* 1:e14–e23. [https://doi.org/10.1016/S2666-5247\(20\)30004-5](https://doi.org/10.1016/S2666-5247(20)30004-5).
  38. Jonsdottir HR, Dijkman R. 2016. Coronaviruses and the human airway: a universal system for virus-host interaction studies. *Virology* 13:24. <https://doi.org/10.1186/s12985-016-0479-5>.
  39. Cao X, Coyle JP, Xiong R, Wang Y, Heflich RH, Ren B, Gwinn WM, Hayden P, Rojanasakul L. 2021. Invited review: human air-liquid-interface organotypic airway tissue models derived from primary tracheobronchial epithelial cells—overview and perspectives. *In Vitro Cell Dev Biol Anim* 57:104–132. <https://doi.org/10.1007/s11626-020-00517-7>.
  40. Jia HP, Look DC, Shi L, Hickey M, Pewe L, Netland J, Farzan M, Wohlford-Lenane C, Perlman S, McCray PB, Jr. 2005. ACE2 receptor expression and severe acute respiratory syndrome coronavirus infection depend on differentiation of human airway epithelia. *J Virol* 79:14614–14621. <https://doi.org/10.1128/JVI.79.23.14614-14621.2005>.
  41. Sims AC, Burkett SE, Yount B, Pickles RJ. 2008. SARS-CoV replication and pathogenesis in an *in vitro* model of the human conducting airway epithelium. *Virus Res* 133:33–44. <https://doi.org/10.1016/j.virusres.2007.03.013>.
  42. Ellen BMT, Dinesh Kumar N, Bouma EM, Troost B, Van de Pol DPI, van der Ende-Metselaar HH, Apperloo L, Gosliga DV, van den Berge M, Nawijn MC, van der Voort PHJ, Moser J, Rodenhuis-Zybert IA, Smit JM. 2021. Resveratrol and pterostilbene inhibit SARS-CoV-2 replication in air liquid interface cultured human primary bronchial epithelial cells. *Viruses* 13:1335. <https://doi.org/10.3390/v13071335>.
  43. Wagstaff KM, Rawlinson SM, Hearn AC, Jans DA. 2011. An AlphaScreen (R)-based assay for high-throughput screening for specific inhibitors of nuclear import. *J Biomol Screen* 16:192–200. <https://doi.org/10.1177/1087057110390360>.
  44. Mastrangelo E, Pezzullo M, De Burghgraeve T, Kaptein S, Pastorino B, Dallmeier K, de Lamballerie X, Neyts J, Hanson AM, Frick DN, Bolognesi M, Milani M. 2012. Ivermectin is a potent inhibitor of flavivirus replication specifically targeting NS3 helicase activity: new prospects for an old drug. *J Antimicrob Chemother* 67:1884–1894. <https://doi.org/10.1093/jac/dks147>.
  45. Okumuş N, Demirtürk N, Çetinkaya RA, Güner R, Avcı İY, Orhan S, Konya P, Şaylan B, Karalezli A, Yamanel L, Kayaaslan B, Yılmaz G, Savaşçı U, Eser F, Taşkın G. 2021. Evaluation of the effectiveness and safety of adding ivermectin to treatment in severe COVID-19 patients. *Res Square Preprint* <https://doi.org/10.21203/rs.3.rs-224203/v1>.
  46. Podder CS, Chowdhury N, Sina MI, Haque WMMU. 2020. Outcome of ivermectin treated mild to moderate COVID-19 cases: a single-center, open-label, randomised controlled study. *IMC J Medical Science* 14:1–8.
  47. Hashim HA, Maulood M, Rasheed AM, Fatak DF, Kabah KK, Abdulamir AS. 2020. Controlled randomized clinical trial on using ivermectin with doxycycline for treating COVID-19 patients in Baghdad. *Iraq medRxiv Preprint* <https://doi.org/10.1101/2020.10.26.20219345>.
  48. Chowdhury A, Shahbaz M, Karim MR. 2020. A Randomized Trial of Ivermectin-Doxycycline and Hydroxychloroquine-Azithromycin therapy on COVID-19 patients. *Preprint Research Square*.
  49. Rajter JC, Sherman MS, Fatteh N, Vogel F, Sacks J, Rajter JJ. 2021. Use of ivermectin is associated with lower mortality in hospitalized patients with coronavirus disease 2019: the ivermectin in COVID nineteen Study. *Chest* 159:85–92. <https://doi.org/10.1016/j.chest.2020.10.009>.
  50. Ahmed S, Karim MM, Ross AG, Hossain MS, Clemens JD, Sumiya MK, Phru CS, Rahman M, Zaman K, Somani J, Yasmin R, Hasnat MA, Kabir A, Aziz AB, Khan WA. 2021. A five-day course of ivermectin for the treatment of COVID-19 may reduce the duration of illness. *Int J Infect Dis* 103:214–216. <https://doi.org/10.1016/j.ijid.2020.11.191>.
  51. Soto-Becerra P, Culquichicón C, Hurtado-Roca Y, Araujo-Castillo RV. 2020. Real-world effectiveness of hydroxychloroquine, azithromycin, and ivermectin among hospitalized COVID-19 patients: results of a target trial emulation using observational data from a nationwide healthcare system in Peru. *medRxiv Preprint* <https://doi.org/10.1101/2020.10.06.20208066>.
  52. Ravikirti Roy R, Pattadar C, Raj R, Agarwal N, Biswas B, Majhi PM, Rai DK, Shyama Kumar A, Sarfaraz A. 2021. Ivermectin as a potential treatment for mild to moderate COVID-19 – A double blind randomized placebo-controlled trial. *MedRxiv Preprint* <https://doi.org/10.1101/2021.01.05.21249310>.
  53. Niaee MS, Gheibi N, Namdar P, Allami A, Zolghadr L, Javadi A, Karampour A, Varnaseri M, Bizhani B, Cheraghi F, Naderi Y, Amini F, Karamyan M, Yadyad MJ, Jamshidian R. 2020. Ivermectin as an adjunct treatment for hospitalized adult COVID-19 patients: a randomized multi-center clinical trial. *Res Square Preprint* <https://doi.org/10.21203/rs.3.rs-109670/v1>.
  54. Mohan A, Tiwari P, Suri T, Mittal S, Patel A, Jain A, Velpandian T, Das UA, Bopanna TK, Pandey RM, Shelke S, Singh AR, Bhatnagar S, Masih S, Mahajan S, Dwivedi T, Sahoo B, Pandit A, Bhopale S, Vig S, Gupta R, Madan K, Hadda V, Gupta N, Garg R, Meena VP, Guleria R. 2021. Ivermectin in mild and moderate COVID-19 (RIVET-COV): a randomized, placebo-controlled trial. *Res Square Preprint* <https://doi.org/10.21203/rs.3.rs-191648/v1>.
  55. Lam SD, Bordin N, Waman VP, Scholes HM, Ashford P, Sen N, van Dorp L, Rauer C, Dawson NL, Pang CSM, Abbasian M, Sillitoe I, Edwards SJL, Fraternali F, Lees JG, Santini JM, Orenco CA. 2020. SARS-CoV-2 spike protein predicted to form complexes with host receptor protein orthologues from a broad range of mammals. *Sci Rep* 10:16471. <https://doi.org/10.1038/s41598-020-71936-5>.
  56. Patterson EI, Elia G, Grassi A, Giordano A, Desario C, Medardo M, Smith SL, Anderson ER, Prince T, Patterson GT, Lorusso E, Lucente MS, Lanave G, Lauzi S, Bonfanti U, Stranieri A, Martella V, Solari Basano F, Barrs VR, Radford AD, Agrimi U, Hughes GL, Paltrinieri S, Decaro N. 2020. Evidence of exposure to SARS-CoV-2 in cats and dogs from households in Italy. *Nat Commun* 11:6231. <https://doi.org/10.1038/s41467-020-20097-0>.
  57. Sharun K, Tiwari R, Natesan S, Dhama K. 2020. SARS-CoV-2 infection in farmed minks, associated zoonotic concerns, and importance of the One Health approach during the ongoing COVID-19 pandemic. *Vet Q* <https://doi.org/10.1080/01652176.2020.1867776:1-14>.
  58. Shi J, Wen Z, Zhong G, Yang H, Wang C, Huang B, Liu R, He X, Shuai L, Sun Z, Zhao Y, Liu P, Liang L, Cui P, Wang J, Zhang X, Guan Y, Tan W, Wu G, Chen H, Bu Z. 2020. Susceptibility of ferrets, cats, dogs, and other domesticated animals to SARS-coronavirus 2. *Science* 368:1016–1020. <https://doi.org/10.1126/science.abb7015>.
  59. Oreshkova N, Molenaar RJ, Vreman S, Harders F, Oude Munnink BB, Hakze-van der Honing RW, Gerhards N, Tolsma P, Bouwstra R, Sikkema RS, Tacken MG, de Rooij MM, Weesendorp E, Engelsma MY, Brusckhe CJ, Smit LA, Koopmans M, van der Poel WH, Stegeman A. 2020. SARS-CoV-2 infection in farmed minks, the Netherlands, April and May 2020. *Euro Surveill* 25. <https://doi.org/10.2807/1560-7917.ES.2020.25.23.2001005>.
  60. McAloose D, Laverack M, Wang L, Killian ML, Caserta LC, Yuan F, Mitchell PK, Queen K, Mauldin MR, Cronk BD, Bartlett SL, Sykes JM, Zec S, Stokol T, Ingerman K, Delaney MA, Fredrickson R, Ivancic M, Jenkins-Moore M, Mazingo K, Franzen K, Bergeson NH, Goodman L, Wang H, Fang Y, Olmstead C, McCann C, Thomas P, Goodrich E, Elvinger F, Smith DC, Tong S, Slavinski S, Calle PP, Terio K, Torchetti MK, Diel DG. 2020. From people to *Panthera*: natural SARS-CoV-2 infection in tigers and lions at the Bronx Zoo. *mBio* 11:e02220-20. <https://doi.org/10.1128/mBio.02220-20>.
  61. Gonzalez Canga A, Sahagun Prieto AM, Jose Diez Liebana M, Martinez NF, Vega MS, Vieitez JJ. 2009. The pharmacokinetics and metabolism of ivermectin in domestic animal species. *Vet J* 179:25–37. <https://doi.org/10.1016/j.tvjl.2007.07.011>.
  62. Nolan TJ, Lok JB. 2012. Macrocyclic lactones in the treatment and control of parasitism in small companion animals. *Curr Pharm Biotechnol* 13:1078–1094. <https://doi.org/10.2174/138920112800399167>.
  63. de Melo BAG, Benincasa JC, Cruz EM, Maricato JT, Porcionatto MA. 2020. 3D culture models to study SARS-CoV-2 infectivity and antiviral candidates: From spheroids to bioprinting. *Biomed J* <https://doi.org/10.1016/j.bj.2020.11.009>.

64. Vieira Braga FA, Kar G, Berg M, Carpaij OA, Polanski K, Simon LM, Brouwer S, Gomes T, Hesse L, Jiang J, Fasouli ES, Efremova M, Vento-Tormo R, Talavera-Lopez C, Jonker MR, Affleck K, Palit S, Strzelecka PM, Firth HV, Mahbubani KT, Cvejic A, Meyer KB, Saeb-Parsy K, Luinge M, Brandsma CA, Timens W, Angelidis I, Strunz M, Koppelman GH, van Oosterhout AJ, Schiller HB, Theis FJ, van den Berge M, Nawijn MC, Teichmann SA. 2019. A cellular census of human lungs identifies novel cell states in health and in asthma. *Nat Med* 25: 1153–1163. <https://doi.org/10.1038/s41591-019-0468-5>.
65. Heijink IH, Kies PM, Kauffman HF, Postma DS, van Oosterhout AJ, Vellenga E. 2007. Down-regulation of E-cadherin in human bronchial epithelial cells leads to epidermal growth factor receptor-dependent Th2 cell-promoting activity. *J Immunol* 178:7678–7685. <https://doi.org/10.4049/jimmunol.178.12.7678>.
66. Heijink IH, Postma DS, Noordhoek JA, Broekema M, Kapus A. 2010. House dust mite-promoted epithelial-to-mesenchymal transition in human bronchial epithelium. *Am J Respir Cell Mol Biol* 42:69–79. <https://doi.org/10.1165/rcmb.2008-0449OC>.
67. Stemcell Technologies. 2021. Air-Liquid Interface Culture for Respiratory Research, on <https://www.stemcell.com/air-liquid-interface-culture-respiratory-research-lp.html>. Accessed 24 February, 2021.